HHS Public Access

Author manuscript

Optom Vis Sci. Author manuscript; available in PMC 2021 April 28.

Published in final edited form as:

Optom Vis Sci. 2019 August ; 96(8): 599–608. doi:10.1097/OPX.0000000000001408.

Custom Optical Coherence Tomography Parameters for Distinguishing Papilledema from Pseudopapilledema

Laura P. Pardon, OD, MS, FAAO, **Han Cheng, OD, PhD**, **Rosa A. Tang, MD**, **Roberto Saenz, OD, MS, FAAO**, **Laura J. Frishman, PhD, FAAO**, **Nimesh B. Patel, OD, PhD, FAAO**

College of Optometry, University of Houston, Houston, TX

Abstract

Significance: Causes of papilledema can be life-threatening, however, distinguishing papilledema from pseudopapilledema is often challenging. The standard conventional optical coherence tomography (OCT) scan for assessing the optic nerve often fails to detect mild papilledema. Our study suggests that parameters derived from volumetric OCT scans can provide additional useful information for detecting papilledema.

Purpose: OCT analysis of the optic nerve commonly measures retinal nerve fiber layer thickness (RNFLT) along a 1.73-mm radius scan path. This conventional scan, however, often fails to detect mild papilledema. The purpose of this study was to evaluate additional OCT-derived measures of the optic nerve head (ONH) and peripapillary retina for differentiating papilledema (all grades and mild) from pseudopapilledema.

Methods: Cirrus OCT ONH volume scans were acquired from 21 papilledema (15 mild papilledema), 27 pseudopapilledema, and 42 control subjects. Raw scan data were exported, and total retinal thickness (TRT) within Bruch's membrane opening (BMO) plus RNFLT and TRT at the following eccentricities were calculated using custom algorithms: BMO to 250 μm, 250–500 μm, 500–1000 μm, and 1000–1500 μm. Minimum rim width (MRW) was calculated, and BMO height was measured from a 4-mm Bruch's membrane reference plane centered on the BMO.

Results: RNFLT from BMO to 250 μm, MRW, and BMO height had significantly greater areas under the receiver operating characteristic curve than that of conventional RNFLT for differentiating mild papilledema from pseudopapilledema ($P < 0.0001$) and greater sensitivities at 95% specificity. Using cutoff values at 95% specificity, custom parameters detected 10 mild papilledema patients and conventional RNFLT detected only one. BMO heights above the reference plane were observed in papilledema only, although many papilledema cases had a neutral or negative BMO height.

Conclusions: Using OCT volumetric data, additional parameters describing peripapillary tissue thickness, neuroretinal rim thickness, and ONH position can be calculated and provide valuable measures for differentiating mild papilledema from pseudopapilledema.

Correspondence: Laura Pardon, OD, MS, FAAO, College of Optometry, University of Houston, 4901 Calhoun Road, Houston, TX 77204-2020, Telephone: 713-743-6401, Lppardon@central.uh.edu.

INTRODUCTION

Differentiating papilledema, or optic disc edema secondary to elevated intracranial pressure, from less life/sight-threatening causes of optic nerve head elevation and blurred disc margins (i.e., pseudopapilledema) can be challenging in clinical practice.[1] This distinction is especially difficult when optic disc edema is mild in severity. It is imperative to distinguish between the two conditions, however, as papilledema generally warrants prompt additional testing and may result from life-threatening causes, whereas pseudopapilledema typically does not.

Elevated intracranial pressure generally results in distinctive anatomical changes to the optic nerve head and surrounding structures, which should be quantifiable using optical coherence tomography. While several advances in optical coherence tomography imaging and analysis have enhanced clinical care, algorithms for optic nerve analysis are typically aimed towards glaucoma diagnosis and management rather than optic disc edema. For example, the conventional 1.73 mm radius retinal nerve fiber layer scan, while beneficial for moderate or greater disc edema, cannot reliably differentiate between mild papilledema and pseudopapilledema.[2–7] Although alternate quantitative and qualitative metrics such as total retinal thickness in the peripapillary area, neuroretinal rim measures, and retinal pigment epithelium angle have been shown to improve detection, they are not standardized.[8–10] In order to facilitate the clinical diagnosis of papilledema and the ability to closely monitor subtle changes in disc edema over time, it is necessary to develop new optical coherence tomography algorithms that are sensitive to these early changes in optic disc edema.

The goal of the present study was to determine whether optical coherence tomography parameters describing immediate peripapillary tissue thickness, neuroretinal rim tissue thickness, and anterior deflection of the retinal pigment epithelium are useful in differentiating papilledema from pseudopapilledema and normal controls. The performance of these parameters in differentiating papilledema from pseudopapilledema was compared with that of the conventional retinal nerve fiber layer circular scan. The parameters' abilities to distinguish mild papilledema from pseudopapilledema were also assessed, as this distinction is the most difficult.

METHODS

Subjects

A retrospective review of medical records from 2013 to 2015, obtained from the MS Eye CARE Clinic at the University of Houston, identified 21 papilledema and 27 pseudopapilledema patients who had been referred to neuro-ophthalmology to rule out presumed papilledema. These subjects were part of a prior study investigating the use of ultrasonography measurements of optic nerve sheath diameter and optical coherence tomography conventional retinal nerve fiber layer thickness for differentiating papilledema from pseudopapilledema,[11] however, the present analysis differs in the selection criteria for eyes analyzed and in that all optical coherence tomography parameters, including conventional retinal nerve fiber layer thickness, were calculated using custom algorithms. All papilledema patients had a diagnosis of idiopathic intracranial hypertension following

lumbar puncture and magnetic resonance imaging, based on the modified Dandy criteria.[12] Of the 27 pseudopapilledema patients, 11 were diagnosed with buried optic nerve head drusen and 16 were diagnosed with tilted/torted optic nerves. Buried drusen of any depth could potentially affect retinal nerve fiber layer or optic nerve head parameters due to displacement of and/or biomechanical effects on retinal ganglion cell axons; since these are potential findings, this group was included in our analysis in addition to normal controls. Forty-two control subjects, recruited from the University of Houston College of Optometry staff, student, and patient populations, were also included in the study. Control subjects underwent a screening that included visual acuity, intraocular pressure, standard automated perimetry, and ocular health assessment with dilated fundus examination. This study was approved by the Committee for Protection of Human Subjects at the University of Houston and adhered to the tenets of the Declaration of Helsinki. Written informed consent was obtained from all control subjects after explanation of the nature and possible consequences of the study.

All papilledema and pseudopapilledema patients had a thorough initial examination including dilated fundus exam with optic nerve head evaluation by an experienced neuro-ophthalmologist, optical coherence tomography, and ocular ultrasonography. B-scan ultrasonography was used to detect drusen, and standardized A-scan ultrasonography was used to measure optic nerve sheath diameter and to perform the 30-degree test.[13] Further work-up (e.g., magnetic resonance imaging, magnetic resonance venography, lumbar puncture, fluorescein angiography) was performed as needed. Patients were excluded if they had a previous diagnosis of papilledema or any ocular or systemic conditions known to affect the optic nerve.

Optical Coherence Tomography Scan Acquisition and Custom Analysis

Optic Disc Cube 200 × 200 Protocol—Cirrus HD optical coherence tomography (Carl Zeiss Meditec, Dublin, CA) was used for image acquisition. The Optic Disc Cube 200 × 200 protocol was performed to obtain volumetric data for a 20 × 20 degree region. Nominal transverse scaling of 6 mm / 20 degrees (300 μm / degree) and axial scaling of 2 mm / 1024 pixels were used. All analyzed scans had a signal strength of ≥ 7 and good centration, and the reconstructed *en face* OCT image and thickness maps (retinal nerve fiber layer and total retinal thickness) were visually inspected for artifacts or instrument algorithm segmentation errors that might affect measurements.

Optical coherence tomography data, including reflectance values and instrument-derived retinal nerve fiber layer thickness and total retinal thickness measures, were exported (img and Advanced Export), and custom algorithms (programmed in MATLAB, The Mathworks Inc., Natick, MA) were used to read in the data and perform further analysis.

The center of the optic nerve head was manually selected on a two-dimensional *en face* image. Subsequently, twelve equally spaced radial sections, corresponding with “clock hour” and “half hour” positions, were automatically interpolated from the volumetric data using this center. Radial B-scans were compensated to facilitate Bruch’s membrane opening identification.[14] The points corresponding with Bruch’s membrane opening were manually selected on each radial scan. Radial scans were used to calculate optic nerve head rim tissue

thickness and displacement, whereas peripapillary tissue thickness measures were calculated from volumetric data. Analysis for our custom parameters was performed as described below.

Peripapillary Tissue Thickness—In papilledema, the immediate peripapillary tissue thickens prior to more distal regions, such as that sampled by the conventional circular retinal nerve fiber layer scan. Although the retinal nerve fiber layer is the primary retinal site affected in papilledema,[15] this layer becomes difficult to segment at eccentricities close to the disc margin in the presence of edema. Average total retinal thickness is less prone to segmentation errors and has been described as performing favorably compared to average retinal nerve fiber layer thickness in detecting papilledema.[8,16] We therefore chose to investigate both retinal nerve fiber layer thickness and total retinal thickness.

Selected Bruch's membrane opening points were fit with an ellipse, and concentric ellipses at increasing eccentricities (250, 500, 1000 and 1500 μm) from Bruch's membrane opening were created. Subsequently, 5 annular zones were used for determining average peripapillary thickness measures (Fig. 1A): (1) within the Bruch's membrane opening ellipse, (2) Bruch's membrane opening ellipse to 250 μm, (3) 250 to 500 μm, (4) 500 to 1000 μm, and (5) 1000 to 1500 μm. Only total retinal thickness was measured within the Bruch's membrane opening ellipse, as the neuronal tissue within the ellipse consists primarily of ganglion cell axons and segmentation of retinal layers was therefore not appropriate. Conventional retinal nerve fiber layer thickness was calculated as the average retinal nerve fiber layer thickness along a 1.73 mm radius circular scan path with its origin at the center of the Bruch's membrane opening points; this differs from the custom thickness measures, which were measured a given distance from the Bruch's membrane opening ellipse rather than the center of the disc. The instrument-derived retinal nerve fiber layer and total retinal thickness segmentation data contained in the exported raw files were used to obtain all thickness measures.

Optic Nerve Head Rim Tissue Thickness—Neuroretinal rim tissue thickness has demonstrated greater sensitivity for identifying papilledema compared with the conventional retinal nerve fiber layer thickness scan.[9] The neuroretinal rim can be quantified using different metrics (e.g., horizontal/vertical/minimum rim width, neuroretinal rim volume) and is also dependent on segmentation and retinal scaling for the instrument. Minimum rim width is a sensitive measure for detecting early glaucomatous changes,[17–22] and we hypothesized that it would also be sensitive to changes associated with mild disc edema. Minimum rim width is not nominally quantified on Cirrus optic nerve head volume scans. For the present analysis, the minimum rim width was quantified as the minimum scaled distance from Bruch's membrane opening to the internal limiting membrane on each interpolated radial scan (Fig. 1B).

Optic Nerve Head Displacement—Anterior deflection of the retinal pigment epithelium has been reported as being specific to papilledema and is thought to occur due to an increased pressure gradient across the lamina cribrosa in the presence of elevated intracranial pressure.[10] Typically, the angle of deflection is referenced to a tangential line from a distal, non-deformed region of the retinal pigment epithelium/Bruch's membrane.

While this metric is useful for moderate cases of retinal pigment epithelium deformation, inward deflection may be more subtle and difficult to appreciate in mild cases. To standardize this measure, a 4 mm Bruch's membrane reference plane centered on the optic nerve was used; this was a linear plane fit to the 24 Bruch's membrane points selected 2 mm from the Bruch's membrane opening center (two for each of the 12 radial B-scans). An eccentricity of 2 mm was selected because there is generally minimal bowing/distortion at this location. Retinal pigment epithelium deflection was quantified as the Bruch's membrane opening height referenced to this plane (Fig. 1B). Bruch's membrane opening height was calculated as the perpendicular distance along the z-axis from the reference plane to each Bruch's membrane opening point in three-dimensional space. Bruch's membrane opening points above the reference plane were defined as having a positive height.

Statistical Analysis

For statistical analysis, the eye with lesser conventional retinal nerve fiber layer thickness was selected for papilledema subjects, and the eye with greater conventional retinal nerve fiber layer thickness was used for pseudopapilledema subjects. Selecting eyes in this manner created the greatest potential for overlap in the distributions of quantitative parameters, thereby making it more difficult to distinguish between the two groups. Data for both eyes of papilledema and pseudopapilledema subjects are presented in the appendix. For control subjects, one eye was selected at random for data acquisition and analysis.

Statistical analysis was performed using GraphPad Prism 7 (GraphPad Software, Inc., San Diego, CA). Several of our custom parameters were not normally distributed, so non-parametric statistical tests were used. The Mann-Whitney *U* test was performed to compare differences between control, pseudopapilledema, and papilledema groups. Differences between mild papilledema and pseudopapilledema were also compared. Global values for each parameter are presented as median (interquartile range). Significance was adjusted to $P = 0.0125$ to account for multiple comparisons (n = 4).

Receiver operating characteristic curve analysis compared the performance of custom parameters to that of conventional retinal nerve fiber layer thickness in differentiating papilledema from pseudopapilledema by comparing areas under curves using SigmaPlot 12.0 (Systat Software, San Jose, CA). Separate analyses were performed for differentiating pseudopapilledema from all grades of papilledema and from mild papilledema only. Using a fixed specificity criterion of 95%, the corresponding sensitivities and cut-off values were determined for representative parameters with the greatest area under the curve. A high specificity was chosen to maximize the number of correctly identified individuals with pseudopapillema, and not papilledema (i.e., those that do not require further work-up). The McNemar test was used to further assess diagnostic ability of custom parameters (GraphPad).

Though our sample size was limited to subjects included in a previous retrospective review, [11] we performed a *post hoc* power calculation in order to ensure that our sample size was adequate. For type I error = 0.05, power = 0.8, and area under the receiver operating characteristic curve = 0.78 (the value for conventional retinal nerve fiber layer thickness in

the present study), the necessary sample sizes for case and control are 12 subjects each; all of our groups included greater than 12 subjects.

RESULTS

Twenty-one of the 48 patients referred to neuro-ophthalmology for presumed papilledema were diagnosed with papilledema secondary to idiopathic intracranial hypertension. The Frisén scale (ranging from 0 to 5) was used to grade papilledema severity based on fundoscopic appearance of the optic nerve head;[23] the present study included subjects with Frisén grades 1 (n = 6), 2 (n = 9), 3 (n = 4), and 4 (n = 2). Fifteen papilledema subjects were therefore described as having mild papilledema (Frisén grades 1 or 2). Median ages for control, pseudopapilledema, papilledema (all grades), and mild papilledema groups were 25.3 (23.8–40.4), 26.7 (18.1–37.5), 26.4 (20.6–35.0), and 32.1 (24.0–38.0) years, respectively. There was a much larger proportion of females:males in the papilledema groups (all grades 19:2, mild papilledema 15:0) than the other two groups (control 25:17, pseudopapilledema 13:14).

Conventional Circumpapillary Retinal Nerve Fiber Layer Thickness

Conventional retinal nerve fiber layer thickness for control, pseudopapilledema, and papilledema groups are shown in Table 1. Comparisons between control and pseudopapilledema ($P = 0.009$), control and papilledema ($P < 0.0001$), and pseudopapilledema and papilledema ($P = 0.0006$) were statistically significant. The retinal nerve fiber layer thickness of subjects with mild papilledema did not differ significantly from that of subjects with pseudopapilledema ($P = 0.03$), suggesting that the conventional clinical scan is not able to distinguish mild papilledema from pseudopapilledema.

Custom Retinal Nerve Fiber Layer and Total Retinal Thickness

Retinal nerve fiber layer thickness and total retinal thickness measures outside the Bruch's membrane opening ellipse decreased with increasing eccentricity for all three groups (Table 1, Fig. 2). Retinal nerve fiber layer thickness was significantly greater in papilledema than pseudopapilledema or controls at all eccentricities ($P < 0.005$, Fig. 2A). Mild papilledema demonstrated a significantly greater retinal nerve fiber layer thickness than pseudopapilledema out to 1000 μm ($P < 0.005$, Fig. 2B); there was no significant difference in retinal nerve fiber layer thickness between these two groups from 1000 to 1500 μm ($P = 0.09$).

Total retinal thickness was significantly greater in papilledema than pseudopapilledema at all eccentricities ($P < 0.005$), however, papilledema only differed from controls out to an eccentricity of 1000 μm ($P < 0.005$, Fig. 2C). Mild papilledema had a significantly greater total retinal thickness than pseudopapilledema from Bruch's membrane opening to 1500 μm ($P < 0.0125$, Fig. 2D); there was no significant difference in total retinal thickness between these two groups within Bruch's membrane opening ($P = 0.10$).

Minimum Rim Width

Minimum rim width values for control, pseudopapilledema, and papilledema groups were 345.5 (278.8–394.5) μm, 478.3 (410.7–517.5) μm, and 576.7 (518.5–687.4) μm, respectively (Fig. 3A). All three comparisons between groups were statistically significant ($P < 0.0001$). Mild papilledema subjects had a median minimum rim width of 546 (504.5–580.8) μm, which was significantly greater than that of the pseudopapilledema group ($P = 0.006$; Fig. 3B).

Bruch's Membrane Opening Height

The median Bruch's membrane opening heights for control, pseudopapilledema, and papilledema groups were −108.4 (−160.7 to −79.64) μm, −106.3 (−138.4 to −56.63) μm, and −6.7 (−56.4 to +18.94) μm, respectively (Fig. 3C). While papilledema subjects had a significantly greater (more positive) height compared with control or pseudopapilledema groups ($P < 0.0001$), there was no significant difference between control and pseudopapilledema ($P = 0.31$). Although the median value represents a height slightly below the reference plane, 9/21 (43%) papilledema subjects had Bruch's membrane opening heights that were above the reference plane, or positive. No control or pseudopapilledema subjects had a positive Bruch's membrane opening height.

In mild papilledema, the median Bruch's membrane opening height was −7.0 (−59.2 to +15.8) μm (Fig. 3D), similar to the median and interquartile range for all grades of papilledema. In total, 6/15 (40%) mild papilledema subjects had positive Bruch's membrane opening heights. Bruch's membrane opening height remained significantly greater when comparing mild papilledema to pseudopapilledema ($P < 0.0001$).

Receiver Operating Characteristic Curve Analysis

Conventional retinal nerve fiber layer thickness had an area under the receiver operating characteristic curve of 0.78 for differentiating all grades of papilledema from pseudopapilledema and 0.70 for differentiating mild papilledema from pseudopapilledema. Sensitivity and cutoff values at 95% specificity for conventional retinal nerve fiber layer thickness and select custom parameters are listed in Table 2. For peripapillary thickness measures, only the eccentricity from Bruch's membrane opening to 250 μm was included in the analysis since the difference between papilledema and pseudopapilledema was greatest at this location.

The area under the curve was significantly increased when Bruch's membrane opening height (0.90) or minimum rim width (0.82) were used to differentiate all grades of papilledema from pseudopapilledema ($P < 0.0001$). For differentiating mild papilledema from pseudopapilledema, Bruch's membrane opening height, retinal nerve fiber layer thickness from Bruch's membrane opening to 250 μm, and minimum rim width all demonstrated significantly greater areas under the curve (0.89, 0.80, and 0.76, respectively) than that of conventional retinal nerve fiber layer thickness ($P < 0.0001$).

In Figure 4, Venn diagrams illustrate the overlap of these three custom parameters exceeding their respective thresholds at 95% specificity for individual subjects. All papilledema

subjects with Frisén grade 3 or greater had at least two of the three custom parameters, as well as conventional retinal nerve fiber layer thickness, above threshold. In mild papilledema, 10 (67%) cases demonstrated at least one elevated custom parameter; specifically, 8 (53%) demonstrated an elevated Bruch's membrane opening height, 5 (33%) showed elevated retinal nerve fiber layer thickness from Bruch's membrane opening to 250 μm (3 of which also had a Bruch's membrane opening height above threshold), and 3 (20%) had an elevated minimum rim width (all of which had an elevated retinal nerve fiber layer thickness out to 250 μm). In contrast, conventional retinal nerve fiber layer thickness was only above the 95% specificity cutoff in a single case of mild papilledema; in this case, all three custom parameters exceeded their thresholds. Only 2 (7%) of the pseudopapilledema subjects demonstrated elevated custom parameters; one had a Bruch's membrane opening height that was only 0.2 degrees above the cutoff, and the other had an elevated minimum rim width and retinal nerve fiber layer thickness (both from Bruch's membrane opening to 250 μm and conventional). For the two metrics that identified the majority of mild papilledema cases, a McNemar test was performed. This test determined that a significantly greater proportion of cases was detected using Bruch's membrane opening height than conventional retinal nerve fiber layer thickness ($P = 0.02$), however the proportion of cases detected using retinal nerve fiber layer thickness from Bruch's membrane opening to 250 μm was not significantly greater than conventional retinal nerve fiber layer thickness ($P = 0.13$).

DISCUSSION

The pathophysiology of papilledema involves swelling of retinal ganglion cell axons due to axoplasmic flow stasis. Prior studies have suggested that this edema originates at the prelaminar region and optic nerve head prior to affecting the peripapillary retina.[15] Quantifying optical coherence tomography parameters at or near these regions that are first affected should therefore enhance our ability to detect early or mild papilledema compared with the conventional 1.73 mm radius retinal nerve fiber layer scan. The results of the present study support this hypothesis. While there was no significant difference in retinal nerve fiber layer thickness between mild papilledema and pseudopapilledema subjects using the conventional circular scan, there was a significant difference in peripapillary tissue thickness measures at eccentricities closer to the optic nerve head. Minimum rim width and Bruch's membrane opening height were also significantly greater in mild papilledema than pseudopapilledema.

Minimum rim width and retinal nerve fiber layer thickness measures adjacent to the optic nerve head are useful parameters for differentiating papilledema from pseudopapilledema, as they provide quantitative information regarding structures at or near the initial site of axoplasmic flow stasis and edema. Our Venn diagrams showed that retinal nerve fiber layer thickness at the innermost eccentricity detected 5 (33%) of the mild papilledema cases, whereas the conventional retinal nerve fiber layer thickness only detected one. Additionally, two mild papilledema subjects below threshold for Bruch's membrane opening height had both a minimum rim width and retinal nerve fiber layer thickness at the innermost eccentricity above the cutoff value at 95% specificity. Though previous studies have found total retinal thickness to perform better than retinal nerve fiber layer thickness,[8,10] the

present study found that retinal nerve fiber layer thickness was better able to distinguish mild papilledema from pseudopapilledema than total retinal thickness, based on it having a significantly greater area under the receiver operating characteristic curve compared with conventional retinal nerve fiber layer thickness and a higher sensitivity at 95% specificity, as demonstrated in Table 2. While conventional retinal nerve fiber layer thickness did not significantly differ between mild papilledema and pseudopapilledema, our custom retinal nerve fiber layer thickness parameters did significantly differ out to an eccentricity of 1000 μm. In individuals with a typical optic disc size, the conventional scan is generally located within the annulus from 1000 to 1500 μm. This indicates that measuring retinal nerve fiber layer thickness at eccentricities closer to the optic nerve head, where disc edema originates, improves detection of papilledema compared with more distal measures, as is currently the standard.

Bruch's membrane opening height emerges as a particularly useful parameter for differentiating papilledema from pseudopapilledema. In addition to Bruch's membrane opening height having the highest sensitivity at 95% specificity, a positive height was highly specific for papilledema. In five (33%) mild papilledema patients, Bruch's membrane opening height was the only parameter that exceeded the cutoff value at 95% specificity, suggesting that anterior deflection of the retinal pigment epithelium may be one of the first manifestations of papilledema in some individuals. In three additional mild papilledema patients (20%), Bruch's membrane opening height and at least one other custom parameter exceeded the 95% cutoff value. It is logical that an anterior deflection of the retinal pigment epithelium would also result in an increase in the Bruch's membrane opening horizontal transverse diameter; this parameter has also recently been described as useful for differentiating mild papilledema from pseudopapilledema.[24]

Our finding that 43% of all papilledema subjects have a positive Bruch's membrane opening height is slightly less than the 67% of papilledema subjects with a positive retinal pigment epithelium deflection reported by Kupersmith et al.[10] This could potentially be explained by the relatively large proportion of individuals with mild papilledema included in the present study and our selection of papilledema eyes with the thinnest retinal nerve fiber layer thickness. While anterior deflection of the retinal pigment epithelium is easily visible in some cases, it can be very subtle and difficult to qualitatively appreciate in others; this highlights the importance of standardizing methods for quantifying the magnitude of deflection. 40% of our mild papilledema subjects had a positive Bruch's membrane opening height using our standardized methods. In contrast, none of our control or pseudopapilledema subjects had a Bruch's membrane opening height that was positive. This suggests that Bruch's membrane opening height is highly specific for differentiating papilledema from pseudopapilledema. Although a neutral or negative height does not rule out papilledema, nerves that exhibit a positive Bruch's membrane opening height should be highly suspicious for disc edema secondary to elevated intracranial pressure. Patients with mild papilledema and pseudopapilledema often present with indistinguishable phenotypes (e.g., blurred optic disc margins, nasal elevation); in these cases, Bruch's membrane opening height can provide valuable additional information and insight whether intracranial pressure is likely to be elevated.

Bruch's membrane opening height quantifies the magnitude of inward displacement of the optic nerve head, which can be explained by biomechanics. The optic nerve head has been analyzed as a biomechanical structure, particularly with regards to intraocular pressure elevation and the pathophysiology of glaucoma.[25–29] Evidence of biomechanical forces in papilledema include reports of globe flattening, expansion of the optic nerve sheath, and the presence of retinal and choroidal folds.[30–33] Recent studies have investigated the role of cerebrospinal fluid pressure on optic nerve head biomechanics, demonstrating that elevating cerebrospinal fluid pressure results in increased deformation of the lamina cribrosa and retrolaminar optic nerve, and that this deformation resolves within weeks following an intervention to lower cerebrospinal fluid pressure.[34,35] Prior experiments in non-human primates have demonstrated that Bruch's membrane opening height changes rapidly in response to 10-minute graded increases and decreases in intraocular pressure;[36] we therefore hypothesize that Bruch's membrane opening height would change rapidly in response to changes in cerebrospinal fluid pressure and, in longitudinal cases, may provide some insight regarding whether cerebrospinal fluid pressure is acutely elevated.

The present study has several limitations. Annular retinal nerve fiber layer thickness and total retinal thickness measures were interpolated from exported instrument-derived segmentation data and therefore may be affected by segmentation errors, especially at higher grades of papilledema. In some cases of moderate-to-severe papilledema, Bruch's membrane opening was difficult to identify due to shadowing from an edematous retinal nerve fiber layer; to facilitate identification of Bruch's membrane opening, all scans were compensated as described in the methods. Additionally, the sample size included is small, with only 15 subjects diagnosed with mild papilledema (6 with Frisén 1). Due to the study's retrospective nature, biometry data were not available for transverse retinal scaling. This is similar to the limitations of clinical practice, however, where there might not be time to obtain biometry and calculate individualized scaling when dealing with an emergent situation such as papilledema. While the focus of this study was on quantitative optical coherence tomography parameters, qualitative signs (e.g., retinal pigment epithelium deformation, subretinal hypo-reflective space), fundus features (e.g., retinal/choroidal folds, hemorrhage, vessel obscuration), and supplementary diagnostic tests (e.g., ultrasonography, fundus autofluorescence, fluorescein angiography) can provide additional useful information for differentiating mild papilledema from pseudopapilledema and should be considered in a clinical work-up.

Minimum rim width is an increasingly popular parameter for detecting early glaucoma and, as a result, software capable of analyzing minimum rim width is presently available on some commercial instruments (e.g., Spectralis Glaucoma Module Premium Edition, Heidelberg Engineering, Germany). Currently, Bruch's membrane opening height and retinal nerve fiber layer and total retinal thickness measures at eccentricities closer to the optic nerve head than a 1.73 mm radius can only be obtained using custom programs. If incorporated into future optical coherence tomography software, these parameters could be obtained and compared to normative ranges rapidly in a clinical setting. Enhanced scan resolution with newer generation instruments may improve accuracy of automated segmentation algorithms, further facilitating the clinical application of these parameters.

In conclusion, optical coherence tomography parameters describing retinal nerve fiber layer thickness adjacent to the optic nerve head, neuroretinal rim thickness, and optic nerve head anterior displacement appear to be more useful than the conventional retinal nerve fiber layer scan for detecting papilledema. A positive Bruch's membrane opening height is highly specific for papilledema, as no control or pseudopapilledema subjects had a Bruch's membrane opening height above the reference plane. Despite its favorable performance compared with other optical coherence tomography parameters, Bruch's membrane opening height has limited sensitivity (57% at 95% specificity, missing 43% of cases); while a positive height is indicative of papilledema, a neutral or negative height does not rule it out and additional work-up to capture all cases of papilledema would be necessary. This study demonstrates that commercial optical coherence tomography analysis techniques could be improved by incorporating additional quantitative parameters to supplement the battery of tests used to detect and monitor optic nerve pathologies.

Support:

NIH T32 EY07024, NIH P30 EY007551

Appendix

Table A1:

Distribution of custom retinal nerve fiber layer and total retinal thickness values for all eyes

Conventional retinal nerve fiber layer thickness, custom retinal nerve fiber layer thickness, and custom total retinal thickness values for control, papilledema, and pseudopapilledema eyes. Papilledema and pseudopapilledema eyes are described as "better" or "worse" depending on which eye had a thicker conventional retinal nerve fiber layer (worse = thicker). In the present study, "better" papilledema eyes were compared to "worse" pseudopapilledema eyes in order to make the two groups more difficult to differentiate. Values for both eyes are included here to provide a more complete clinical picture.

	Retinal Nerve Fiber Layer Thickness Median (Interquartile Range), μm					**Total Retinal Thickness Median (Interquartile Range), μm**				
	Conventional (1.73 mm radius)	**BMO to 250 μm**	**250 to 500 μm**	**500 to 1000 μm**	**1000 to 1500 μm**	**Within BMO**	**BMO to 250 μm**	**250 to 500 μm**	**500 to 1000 μm**	**1000 to 1500 μm**
Control (n = 42)	91.0 (86–96)	168.6 (134–183)	143 (125–156)	105 (100–114)	78.1 (76–83)	201.7 (88–297)	331.8 (297–374)	330.6 (311–348)	312.5 (298–323)	293.7 (285–306)
PE (worse) (n = 21)	231 (105–312)	378.7 (309–456)	267.7 (215–326)	135.8 (121–193)	87.8 (77–100)	833.3 (670–1003)	671.5 (573–735)	503.1 (444–580)	357.3 (338–423)	301.1 (290–313)
PE (better) (n = 21)	128.7 (102–207)	306.2 (262–424)	227.3 (205–342)	130.5 (122–191)	88.1 (82–103)	710.2 (568–911)	612 (517–771)	461.8 (431–585)	351.8 (336–416)	297.4 (289–314)
Mild PE (worse) (n = 15)	107.7 (104–151)	321.1 (297–368)	222 (194–267)	123.5 (118–143)	81 (75–88)	706.1 (651–888)	581.8 (538–645)	460.1 (409–491)	344.4 (330–356)	290 (281–297)

	Retinal Nerve Fiber Layer Thickness Median (Interquartile Range), μm					Total Retinal Thickness Median (Interquartile Range), μm				
	Conventional (1.73 mm radius)	BMO to 250 μm	250 to 500 μm	500 to 1000 μm	1000 to 1500 μm	Within BMO	BMO to 250 μm	250 to 500 μm	500 to 1000 μm	1000 to 1500 μm
Mild PE (better) (n = 15)	109.9 (100–132)	293.6 (260–377)	218 (204–276)	127.6 (120–147)	85.6 (81–90)	618.8 (516–786)	529.8 (503–631)	432.4 (425–498)	341.1 (332–366)	295.5 (285–299)
PPE (worse) (n = 27)	102 (87–107)	213 (177–262)	162 (140–198)	114.1 (100–124)	79.4 (74–88)	548.7 (396–703)	459.1 (418–538)	381.5 (356–410)	322.8 (308–336)	285.1 (274–293)
PPE (better) (n = 27)	99.0 (91–105)	212.2 (164–291)	167.3 (150–200)	116.7 (104–123)	83.9 (74–88)	564.4 (385–667)	498.8 (411–542)	390.5 (368–418)	328 (315–342)	293 (275–300)

BMO = Bruch's membrane opening; PE = papilledema; PPE = pseudopapilledema; worse = eye with thicker conventional retinal nerve fiber layer; better = eye with thinner conventional retinal nerve fiber layer

Table A2:
Minimum rim width and Bruch's membrane opening height for all eyes

Minimum rim width and Bruch's membrane opening height values for control, papilledema, and pseudopapilledema eyes. Eyes described as "worse" have a thicker conventional retinal nerve fiber layer. Values for both eyes of papilledema and pseudopapilledema subjects are included to provide a more complete clinical picture.

	Minimum Rim Width Median (Interquartile Range), μm	Bruch's Membrane Opening Height Median (Interquartile Range), μm
Control (n = 42)	345.5 (279 to 395)	−108.4 (−161 to −80)
PE (worse) (n = 21)	627.1 (561 to 689)	+7.5 (−20 to +19)
PE (better) (n = 21)	576.7 (519 to 687)	−6.7 (−56 to +19)
Mild PE (worse) (n = 15)	575.9 (532 to 617)	−2.3 (−36 to +14)
Mild PE (better) (n = 15)	546 (505 to 581)	−7.0 (−59 to +16)
PPE (worse) (n = 27)	478.3 (411 to 518)	−106.3 (−138 to −57)
PPE (better) (n = 27)	501.9 (402 to 558)	−114 (−171 to −77)

PE = papilledema; PPE = pseudopapilledema; worse = eye with thicker conventional retinal nerve fiber layer; better = eye with thinner conventional retinal nerve fiber layer

REFERENCES

1. Chiang J, Wong E, Whatham A, et al. The Usefulness of Multimodal Imaging for Differentiating Pseudopapilloedema and True Swelling of the Optic Nerve Head: A Review and Case Series. Clin Exp Optom 2015;98:12–24. [PubMed: 25315395]
2. Johnson LN, Diehl ML, Hamm CW, et al. Differentiating Optic Disc Edema from Optic Nerve Head Drusen on Optical Coherence Tomography. Arch Ophthalmol 2009;127:45–9. [PubMed: 19139337]
3. Lee KM, Woo SJ, Hwang JM. Differentiation of Optic Nerve Head Drusen and Optic Disc Edema with Spectral-Domain Optical Coherence Tomography. Ophthalmology 2011;118:971–7. [PubMed: 21211843]
4. Sarac O, Tasci YY, Gurdal C, Can I. Differentiation of Optic Disc Edema from Optic Nerve Head Drusen with Spectral-Domain Optical Coherence Tomography. J Neuroophthalmol 2012;32:207–11. [PubMed: 22473041]

5. Flores-Rodriguez P, Gili P, Martin-Rios MD. Sensitivity and Specificity of Time-Domain and Spectral-Domain Optical Coherence Tomography in Differentiating Optic Nerve Head Drusen and Optic Disc Oedema. Ophthalmic Physiol Opt 2012;32:213–21. [PubMed: 22428958]
6. Kulkarni KM, Pasol J, Rosa PR, Lam BL. Differentiating Mild Papilledema and Buried Optic Nerve Head Drusen Using Spectral Domain Optical Coherence Tomography. Ophthalmology 2014;121:959–63. [PubMed: 24321144]
7. Karam EZ, Hedges TR. Optical Coherence Tomography of the Retinal Nerve Fibre Layer in Mild Papilloedema and Pseudopapilloedema. Br J Ophthalmol 2005;89:294–8. [PubMed: 15722307]
8. Vartin CV, Nguyen AM, Balmitgere T, et al. Detection of Mild Papilloedema Using Spectral Domain Optical Coherence Tomography. Br J Ophthalmol 2012;96:375–9. [PubMed: 21653211]
9. Huang-Link YM, Al-Hawasi A, Oberwahrenbrock T, Jin YP. OCT Measurements of Optic Nerve Head Changes in Idiopathic Intracranial Hypertension. Clin Neurol Neurosurg 2015;130:122–7. [PubMed: 25614195]
10. Kupersmith MJ, Sibony P, Mandel G, et al. Optical Coherence Tomography of the Swollen Optic Nerve Head: Deformation of the Peripapillary Retinal Pigment Epithelium Layer in Papilledema. Invest Ophthalmol Vis Sci 2011;52:6558–64. [PubMed: 21705690]
11. Saenz R, Cheng H, Prager TC, et al. Use of A-Scan Ultrasound and Optical Coherence Tomography to Differentiate Papilledema from Pseudopapilledema. Optom Vis Sci 2017;94:1081–9. [PubMed: 29120977]
12. Smith JL. Whence Pseudotumor Cerebri? J Clin Neuroophthalmol 1985;5:55–6. [PubMed: 3156890]
13. Ossoinig KC. Standardized Echography: Basic Principles, Clinical Applications, and Results. Int Ophthalmol Clin 1979;19:127–210.
14. Girard MJ, Strouthidis NG, Ethier CR, Mari JM. Shadow Removal and Contrast Enhancement in Optical Coherence Tomography Images of the Human Optic Nerve Head. Invest Ophthalmol Vis Sci 2011;52:7738–48. [PubMed: 21551412]
15. Hayreh SS. Pathogenesis of Optic Disc Edema in Raised Intracranial Pressure. Prog Retin Eye Res 2016;50:108–44. [PubMed: 26453995]
16. Scott CJ, Kardon RH, Lee AG, et al. Diagnosis and Grading of Papilledema in Patients with Raised Intracranial Pressure Using Optical Coherence Tomography Vs Clinical Expert Assessment Using a Clinical Staging Scale. Arch Ophthalmol 2010;128:705–11. [PubMed: 20547947]
17. Chauhan BC, O'Leary N, Almobarak FA, et al. Enhanced Detection of Open-Angle Glaucoma with an Anatomically Accurate Optical Coherence Tomography-Derived Neuroretinal Rim Parameter. Ophthalmology 2013;120:535–43. [PubMed: 23265804]
18. Danthurebandara VM, Sharpe GP, Hutchison DM, et al. Enhanced Structure-Function Relationship in Glaucoma with an Anatomically and Geometrically Accurate Neuroretinal Rim Measurement. Invest Ophthalmol Vis Sci 2014;56:98–105. [PubMed: 25503459]
19. Gardiner SK, Ren R, Yang H, et al. A Method to Estimate the Amount of Neuroretinal Rim Tissue in Glaucoma: Comparison with Current Methods for Measuring Rim Area. Am J Ophthalmol 2014;157:540–9 e1–2. [PubMed: 24239775]
20. Ivers KM, Sredar N, Patel NB, et al. In Vivo Changes in Lamina Cribrosa Microarchitecture and Optic Nerve Head Structure in Early Experimental Glaucoma. PLoS One 2015;10:e0134223. [PubMed: 26230993]
21. Patel NB, Sullivan-Mee M, Harwerth RS. The Relationship between Retinal Nerve Fiber Layer Thickness and Optic Nerve Head Neuroretinal Rim Tissue in Glaucoma. Invest Ophthalmol Vis Sci 2014;55:6802–16. [PubMed: 25249610]
22. Reis AS, O'Leary N, Yang H, et al. Influence of Clinically Invisible, but Optical Coherence Tomography Detected, Optic Disc Margin Anatomy on Neuroretinal Rim Evaluation. Invest Ophthalmol Vis Sci 2012;53:1852–60. [PubMed: 22410561]
23. Frisen L Swelling of the Optic Nerve Head: A Staging Scheme. J Neurol Neurosurg Psychiatry 1982;45:13–8. [PubMed: 7062066]
24. Thompson AC, Bhatti MT, El-Dairi MA. Bruch's membrane opening on optical coherence tomography in pediatric papilledema and pseudopapilledema. J AAPOS 2018;22:38–43. [PubMed: 29203329]

25. Burgoyne CF, Downs JC, Bellezza AJ, et al. The Optic Nerve Head as a Biomechanical Structure: A New Paradigm for Understanding the Role of Iop-Related Stress and Strain in the Pathophysiology of Glaucomatous Optic Nerve Head Damage. Prog Retin Eye Res 2005;24:39–73. [PubMed: 15555526]
26. Sigal IA, Ethier CR. Biomechanics of the Optic Nerve Head. Exp Eye Res 2009;88:799–807. [PubMed: 19217902]
27. Sigal IA, Flanagan JG, Ethier CR. Factors Influencing Optic Nerve Head Biomechanics. Invest Ophthalmol Vis Sci 2005;46:4189–99. [PubMed: 16249498]
28. Stowell C, Burgoyne CF, Tamm ER, et al. Biomechanical Aspects of Axonal Damage in Glaucoma: A Brief Review. Exp Eye Res 2017; 157:13–19. [PubMed: 28223180]
29. Downs JC. Optic Nerve Head Biomechanics in Aging and Disease. Exp Eye Res 2015;133:19–29. [PubMed: 25819451]
30. Brodsky MC, Vaphiades M. Magnetic Resonance Imaging in Pseudotumor Cerebri. Ophthalmology 1998;105:1686–93. [PubMed: 9754178]
31. Bidot S, Saindane AM, Peragallo JH, et al. Brain Imaging in Idiopathic Intracranial Hypertension. J Neuroophthalmol 2015;35:400–11. [PubMed: 26457687]
32. Hansen HC, Helmke K. Validation of the Optic Nerve Sheath Response to Changing Cerebrospinal Fluid Pressure: Ultrasound Findings During Intrathecal Infusion Tests. J Neurosurg 1997;87:34–40. [PubMed: 9202262]
33. Sibony PA, Kupersmith MJ, Feldon SE, et al. Retinal and Choroidal Folds in Papilledema. Invest Ophthalmol Vis Sci 2015;56:5670–80. [PubMed: 26335066]
34. Feola AJ, Coudrillier B, Mulvihill J, et al. Deformation of the Lamina Cribrosa and Optic Nerve Due to Changes in Cerebrospinal Fluid Pressure. Invest Ophthalmol Vis Sci 2017;58:2070–8. [PubMed: 28389675]
35. Morgan WH, Chauhan BC, Yu DY, et al. Optic Disc Movement with Variations in Intraocular and Cerebrospinal Fluid Pressure. Invest Ophthalmol Vis Sci 2002;43:3236–42. [PubMed: 12356830]
36. Patel N, McAllister F, Pardon L, Harwerth R. The Effects of Graded Intraocular Pressure Challenge on the Optic Nerve Head. Exp Eye Res 2018;169:79–90. [PubMed: 29409880]

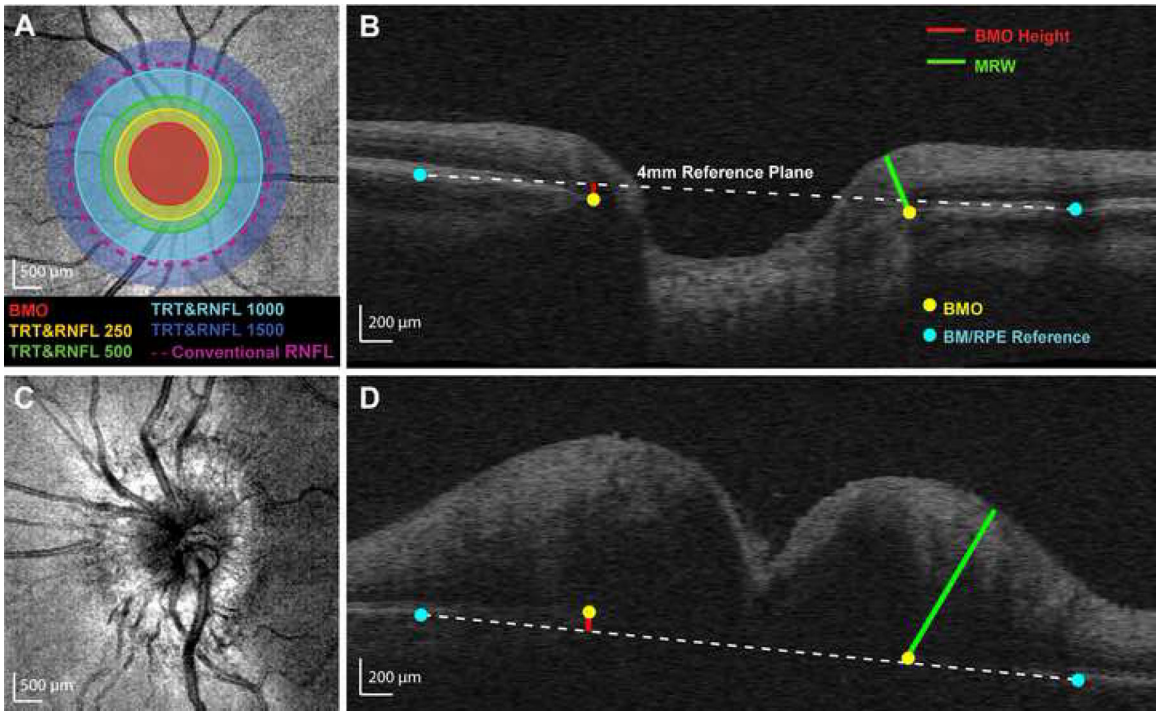

Figure 1.

Calculation of custom parameters. (A) Cirrus optical coherence tomography mean reflectance image of a control eye. Selected Bruch's membrane opening (BMO) points were fit with an ellipse. Five annular zones were used for determining average retinal nerve fiber layer (RNFL) thickness and total retinal thickness (TRT) from volumetric data: (1) within the BMO ellipse (BMO, red), (2) BMO ellipse to 250 µm (RNFL250 and TRT250, yellow), (3) 250 to 500 µm (RNFL500 and TRT500, green), (4) 500 to 1000 µm (RNFL1000 and TRT1000, light blue), and (5) 1000 to 1500 µm (RNFL1500 and TRT1500, dark blue). The conventional RNFL scan (nominally 1730 µm from the center of the optic nerve head, approximately 1100 µm from the BMO in this individual) is represented by the dashed purple line. (B) Control B-scan demonstrating custom optic nerve head (ONH) parameters. Minimum rim width (MRW, green line) was calculated as the minimum distance from BMO (yellow dots) to the internal limiting membrane. A reference plane (white dashed line) was created by connecting points selected at the Bruch's membrane/retinal pigment epithelium interface 2 mm from the ONH center (blue dots) for each interpolated radial scan. BMO height (red line) was calculated as the perpendicular distance from the reference plane to the BMO. (C) Mean reflectance image of an eye with papilledema. (D) B-scan for the same papilledema eye, demonstrating custom ONH parameters. Note that the BMO is above the reference plane in this subject with papilledema.

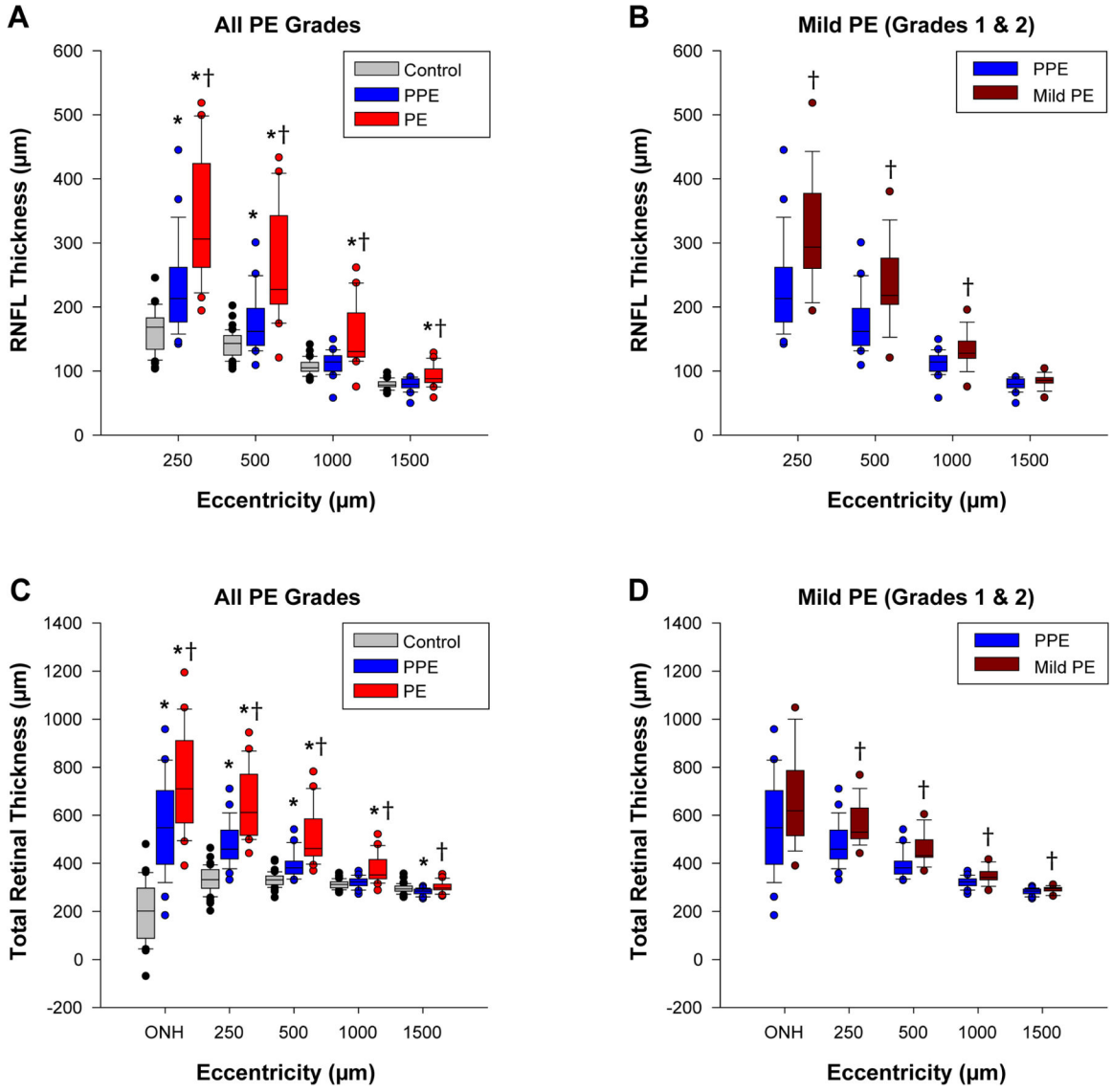

Figure 2.

Retinal nerve fiber layer thickness (RNFLT) and total retinal thickness (TRT) at various eccentricities. Boxes represent the 25th and 75th percentiles, whiskers represent the 10th and 90th percentiles, and the horizontal line depicts the median thickness. (A&B) RNFLT comparisons between groups for all grades of papilledema and mild papilledema. (C&D) TRT comparisons for all grades of papilledema and mild papilledema. *Comparison with control is statistically significant ($P < 0.0125$); †comparison with pseudopapilledema is statistically significant ($P < 0.0125$).

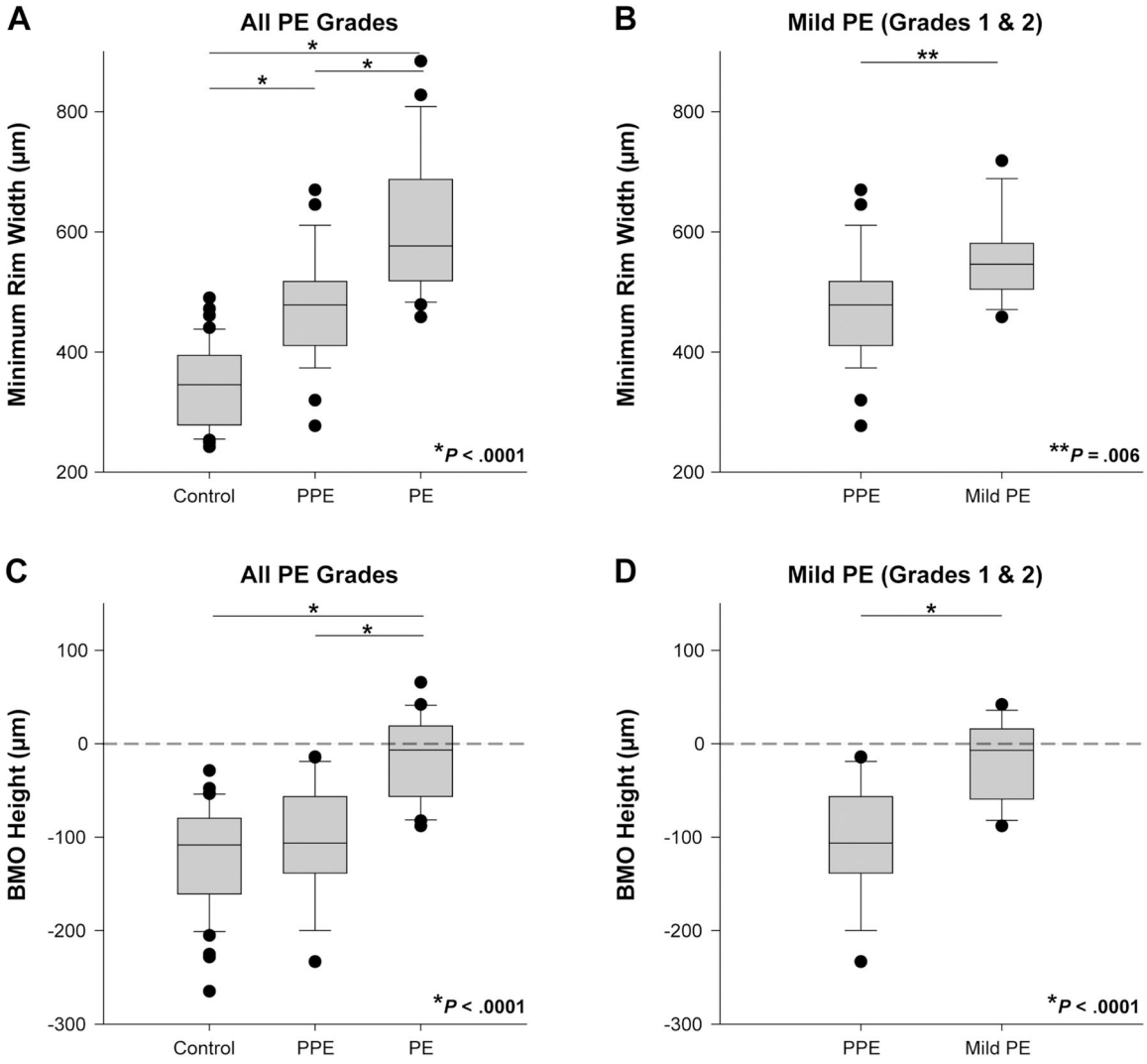

Figure 3.

Minimum rim width (MRW) and Bruch's membrane opening (BMO) height. (A) MRW was greater in papilledema than in controls or pseudopapilledema ($P < 0.0001$). (B) MRW was significantly greater in mild papilledema than pseudopapilledema ($P = 0.006$). (C) BMO height was significantly greater in papilledema compared with pseudopapilledema and control groups ($P < 0.0001$). No control or pseudopapilledema subjects had a positive BMO height. (D) BMO height was significantly greater in mild papilledema than in pseudopapilledema ($P < 0.0001$).

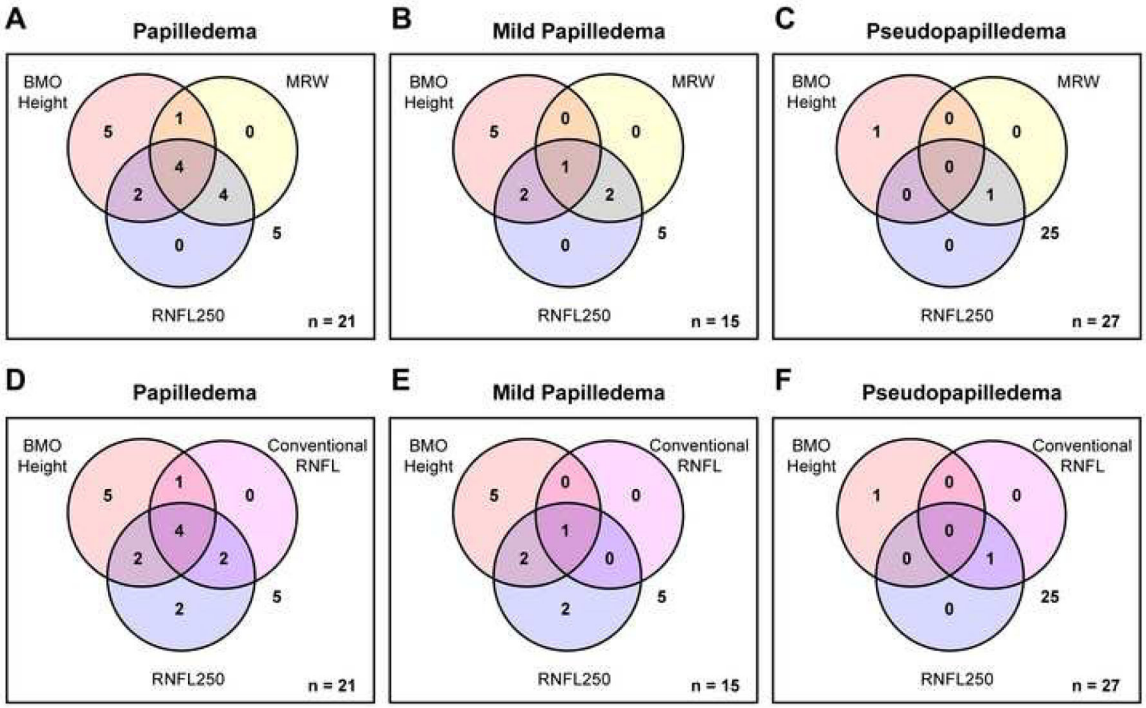

Figure 4.

Venn diagrams depicting overlap of parameters above their respective thresholds at 95% specificity for (A&D) all grades of papilledema (n = 21), (B&E) mild papilledema (n = 15), and (C&F) pseudopapilledema (n = 27). The number of subjects with no measures above 95% specificity is shown to the right of the diagrams. Only a single patient with mild papilledema had a conventional retinal nerve fiber layer thickness above threshold, whereas 10 mild papilledema patients demonstrated at least one elevated custom parameter.

Table 1:

Distribution of custom retinal nerve fiber layer and total retinal thickness values

	Retinal Nerve Fiber Layer Thickness Median (Interquartile Range), µm					Total Retinal Thickness Median (Interquartile Range), µm				
	Conventional (1.73 mm radius)	**BMO to 250 µm**	**250 to 500 µm**	**500 to 1000 µm**	**1000 to 1500 µm**	**Within BMO**	**BMO to 250 µm**	**250 to 500 µm**	**500 to 1000 µm**	**1000 to 1500 µm**
Control (n = 42)	91.0 (86–96)	168.6 (134–183)	143 (125–156)	105 (100–114)	78.1 (76–83)	201.7 (88–297)	331.8 (297–374)	330.6 (311–348)	312.5 (298–323)	293.7 (285–306)
PE (n = 21)	128.7 *† (102–207)	306.2 *† (262–424)	227.3 *† (205–342)	130.5 *† (122–191)	88.1 *† (82–103)	710.2 *† (568–911)	612 *† (517–771)	461.8 *† (431–585)	351.8 *† (336–416)	297.4 † (289–314)
Mild PE (n = 15)	109.9 (100–132)	293.6 † (260–377)	218 † (204–276)	127.6 † (120–147)	85.6 (81–90)	618.8 (516–786)	529.8 † (503–631)	432.4 † (425–498)	341.1 † (332–366)	295.5 † (285–299)
PPE (n = 27)	102 * (87–107)	213 * (177–262)	162 * (140–198)	114.1 (100–124)	79.4 (74–88)	548.7 * (396–703)	459.1 * (418–538)	381.5 * (356–410)	322.8 (308–336)	285.1 * (274–293)

BMO = Bruch's membrane opening; PE = papilledema; PPE = pseudopapilledema;

*Comparison with control is statistically significant ($P < 0.0125$). For mild PE, only statistical comparison with PPE was performed.

†Comparison with PPE is statistically significant ($P < 0.0125$).

Table 2:

Receiver operating characteristic curve analysis

	PE (All Grades, n = 21) vs. PPE (n = 27)				Mild PE (n = 15) vs. PPE (n = 27)			
	AUC Analysis		At 95% Specificity		AUC Analysis		At 95% Specificity	
	AUC ± SE	*P*-value*	Sensitivity	Cutoff Value (μm)	AUC ± SE	*P*-value*	Sensitivity	Cutoff Value (μm)
Conventional (1.73 mm radius) RNFLT	0.78 ± 0.07	N/A	0.33	159.3	0.70 ± 0.09	N/A	0.067	161.4
RNFL250	0.84 ± 0.06	0.42	0.48	369.7	0.80 ± 0.07	< 0.0001	0.33	369.7
TRT250	0.85 ± 0.06	0.34	0.43	653.9	0.79 ± 0.07	0.34	0.20	657.9
MRW	0.82 ± 0.06	< 0.0001	0.43	645.7	0.76 ± 0.08	< 0.0001	0.20	646.5
BMO Height	0.90 ± 0.04	< 0.0001	0.57	−14.2	0.89 ± 0.05	< 0.0001	0.53	−14.2

PE = papilledema; PPE = pseudopapilledema; AUC = area under the curve; SE = standard error; RNFLT = retinal nerve fiber layer thickness; RNFL250 = RNFLT from BMO to 250 μm; TRT250 = total retinal thickness from BMO to 250 μm; MRW = minimum rim width; BMO = Bruch's membrane opening

** P*-value comparing AUC to standard RNFL thickness AUC